ELSEVIER

Ceramics International 27 (2001) 761–765

CERAMICS INTERNATIONAL

www.elsevier.com/locate/ceramint

Processing and phase evolution in low voltage varistor prepared by chemical processing

H. Özkan Toplan*, Yılmaz Karakaş

The University of Sakarya, Engineering Faculty, Metallurgy and Materials Department, Esentepe Campus, 54040 Adapazari, Turkey

Received 12 September 2000; received in revised form 22 November 2000; accepted 25 January 2001

Abstract

A new chemical process has been developed to form a low voltage varistor. The chemistry of process has been analysed and used to produce particles consisting of an intimate mix of ZnO, Zn_2TiO_4 and β-Bi_2O_3 phases. The powder was used to produce low-voltage varistor with useful electrical properties. © 2001 Elsevier Science Ltd and Techna S.r.l. All rights reserved.

Keywords: E. Varistor; Processing; Phase evolution

1. Introduction

Zinc oxide varistors are semiconductive ceramics containing small amounts of other metal oxides (such as Bi_2O_3, CoO, MnO, Sb_2O_3 and Cr_2O_3), exhibiting highly non-linear current–voltage characteristics similar to back-to-back Zener diodes but with much greater current and energy handling capabilities [1,2,3]. Each oxide has a specific function and a variety of phases evolve from the mixture on densification affecting the microstructure and, consequently, the varistor response [4].

Fabrication of ZnO varistors follow standard ceramic techniques. ZnO and other constituents are mixed by milling in a ball mill and dried by spraying. The mixture is pressed to the desired shape usually disc like. The resulting pellets are sintered at high temperature (typically 1000–1400°C) [1]. A simplified flow diagram and the major findings of the microstructural analyse are summarized in Fig. 1. The four basic compounds formed are ZnO, spinel, phrochlore and bismuth-rich phases. The phrochlore disappears at high temperature forming spinel and Bi_2O_3 [5].

The observed current–voltage characteristics of a varistor are often empirically described by the power law relation:

$$J = C(E)^{\alpha} \quad (1)$$

where J is the current density, E the electrical field, α the coefficient of non-linearity and C is a constant that is related with the microstructure [6]. Values of α defined current density are usually quoted along with E_b, breakdown field (in Vmm^{-1} at a defined current density, usually 1 $\text{mA}\cdot\text{cm}^{-2}$) necessary for the current to increase rapidly above the knee of the J–E curve. The value of the breakdown voltage, E_b (in Vmm^{-1}) is related to grain size

$$E_b = V_{gb}N_g = V_{gb}\frac{1000}{d} \quad (2)$$

where V_{gb} is the barrier voltage, N_g the number of grains per mm, and d the average grain diameter in μm. Consequently, fine grained varistors will give a higher E_b at a fixed component size component size assuming barrier voltage is constant [4].

For spark protection in car electronics, low-voltage varistors are applied with breakdown voltage of 22 V. The microstructure of low-voltage ZnO varistors has to be fairly coarse-grained in order to ensure low voltage breakdown voltage [7]. Two principal approaches have been used for making low-voltage varistors. One approach is the classical approach of selecting additives that encouraged grain growth and, in some case, exaggerated grain growth [8]. TiO_2 is commonly used as a grain-growth-enhancing additive. However, when ZnO

---

* Corresponding author. Tel.: +90-264-346-0353; fax: +90-264-346-0351.
E-mail address: toplano@sakarya.edu.tr (H.Ö. Toplan).

PII: S0272-8842(01)00027-X

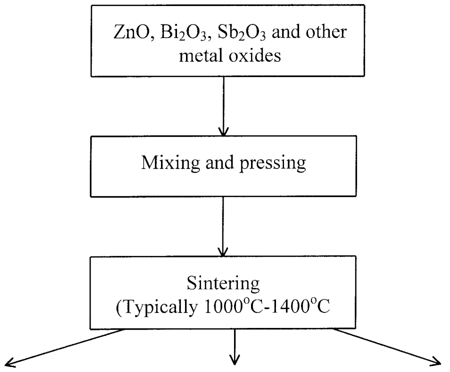

Compound	Chemical Formulation	Doping Element
ZnO	ZnO	Co, Mn
Spinal	$Zn_7Sb_2O_{12}$	Co, Mn, Cr
Pyrochlore	$Bi_{3/2}ZnSb_{3/2}O_7$	Co, Mn, Cr
Bi-rich phase	Bi_2O_3 (α, β, δ and γ)	Zn, Sb

Fig. 1. Simplified flow diagram for the fabrication of ZnO varistors and the major findings of the microstructural analyses [5].

is sintered with small additions of TiO_2, a large spread in grain size due to discontinuous grain growth is often observed [7]. The other is to adopt the approach used in making multilayer capacitors, namely making thin layers by a process such as tape-casting and then stacking up the layers with interdigitated electrodes [8].

In the present work a new chemical process has been developed to form a low voltage varistor. Details of chemistry of the precipitation process are given together with a brief description of microstructural development and electrical behaviour of varistor from this route.

2. Experimental procedure

The starting materials for production of the varistor powder the composition given in Table 1 were reagent grade ZnO, $Bi(NO_3)_3{\cdot}5H_2O$, $Co(NO_3)_2{\cdot}6H_2O$, $MnCl_2{\cdot}4H_2O$ and $Ti(C_2H_5O)_4$. The processing route is shown in Fig. 2. The chemistry of the precipitation process was examined by measuring pH during titration of varistor solution with NaOH + ZnO.

The bulk densities of sintered samples were determined from their weights and dimensions. The characterization of sintered specimens was carried out by X-ray diffraction using CuK_α radiation. Powder morphology were examined using secondary electron imaging (SEI) using a scanning electron microscope (SEM). The phase distribution was revealed by backscatterd electron imaging after polishing and thermally etching for 20 min at 100°C below the sintering temperatures. Grain size measurements were done on the photomicrographs of the etched samples using the following equation.

Table 1
The composition used for precipitation powder varistor

Oxide	ZnO	Bi_2O_3	CoO	MnO	TiO_2
Mol%	97.50	0.5	1.0	0.5	0.50

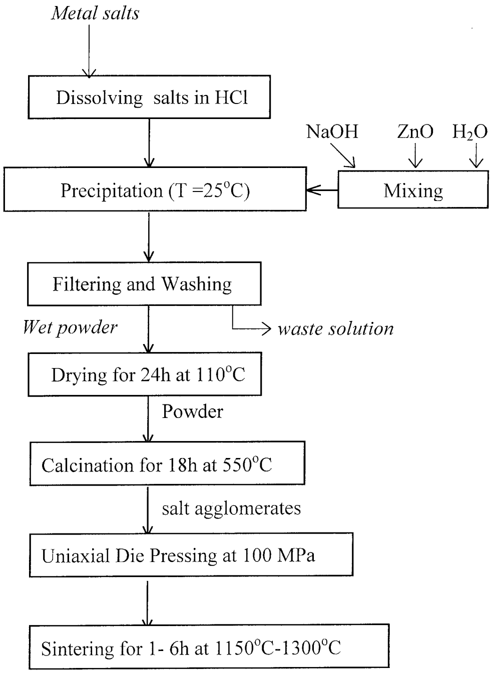

Fig. 2. Block diagrams of the chemical processing route.

$$\bar{G} = 1.56{\cdot}\bar{L} \tag{3}$$

where $\bar{G}$ is the average grain size, $\bar{L}$ is the average grain boundary intercept-length of four random lines on two micrographs [9]. The voltage–current characteristics for samples determined from 10 $\mu A/cm^2$ to 100 mA/cm^2.

3. Results and discussion

Zinc oxide is amphoteric, solube in both acids and bases. When ZnO is added to a NaOH solution, the following reaction partially occurs [10,11]:

$$ZnO + 2NaOH \rightarrow Na_2ZnO_2 + H_2O \tag{4}$$

Then it becomes Na_2ZnO_2 (solution) + ZnO + NaOH (solution) mixture. The other metal salts are dissolved in water with adding HCl to have clear solution. If acid and base solutions are rapidly mixed, the following reactions occur.

$$Bi^{+3} + 3(OH)^- \rightarrow Bi(OH)_3 \downarrow \tag{5}$$

$$Ti^{+4} + 4(OH)^- \rightarrow Ti(OH)_4 \downarrow \tag{6}$$

$$ZnO_2^{-2} + 2H^+ \rightarrow Zn(OH)_2 \rightarrow ZnO \downarrow + H_2O \tag{7}$$

$$Co^{+2} + 2(OH)^- \rightarrow Co(OH)_2 \downarrow \quad (8)$$

$$Mn^{+2} + 2(OH)^- \rightarrow Mn(OH)_2 \downarrow \quad (9)$$

The final product of the process was dried for 24 h at 110°C and calcined at 550°C for 18 h. After such chemical processes, it is well known that a very large surface area, fine and homogeneous morphology can be obtained [4]. This makes the powder easy to sinter.

Fig. 3 shows that the homogeneous primary particles are ranging around 0.5–1 μm arising from the rapidly coprecipitation. However, in common with all prepitated powders, it was agglomerated. Energy dispersive spectroscopy (EDS) analysis suggested that the calcined powder was chemically very homogeneous on the scale of the interaction rang (about 1 μm).

Sung and Kim [12], and Suziki and Bradt [13], have suggested that at below 1030°C TiO_2 rapidly dissolves in the Bi_2O_3-rich liquid phase, reacting with the Bi_2O_3 liquid, and forming the compound $Bi_4Ti_3O_{12}$, according to the following reaction,

$$2Bi_2O_3(l) + 3TiO_2(solution) \rightarrow Bi_4Ti_3O_{12}(s) \quad (10)$$

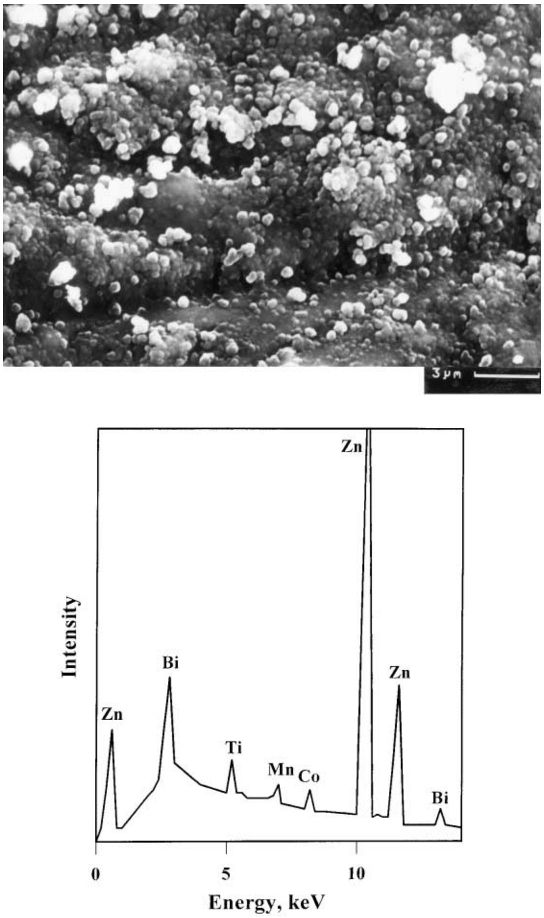

Fig. 3. Secondary electron SEM image of the calcined powder showing very fine morphology and EDS.

The solid $Bi_4Ti_3O_{12}$ is then reported to decompose and react with the solid ZnO grains at ~1050°C, according to the reaction [13,14]

$$Bi_4Ti_3O_{12}(s)+6ZnO(s) \rightarrow 2Bi_2O_3(l) +3Zn_2TiO_4(s) \quad (11)$$

The XRD patterns of 1030 and 1150°C are shown in Fig. 4 (a,b). The presence of the $Bi_4Ti_3O_{12}$ phase is revealed in the sample fired at 1030°C [(a) in Fig. 4], but it disappears after firing at 1150°C and is accompanied

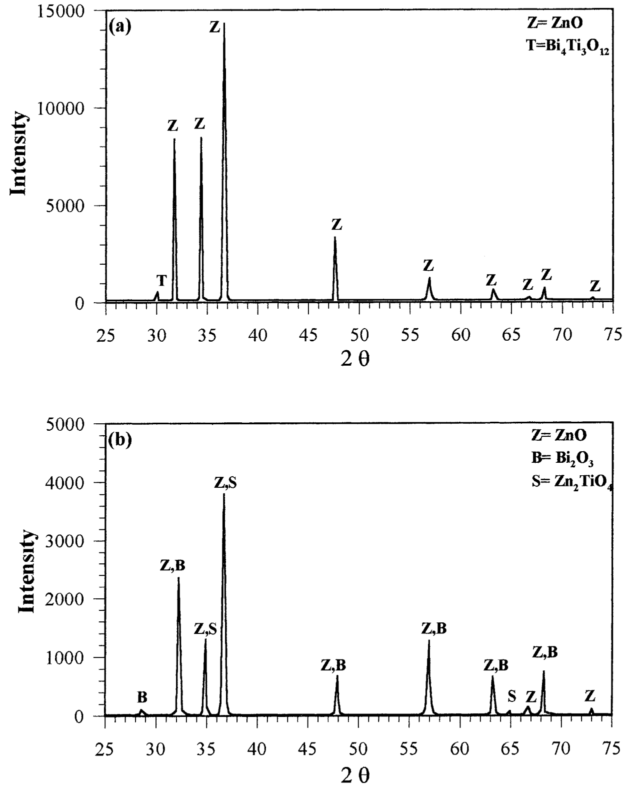

Fig. 4. XRD patterns of the $ZnO{\cdot}Bi_2O_3{\cdot}CoO{\cdot}MnO{\cdot}TiO_2$ samples sintered at (a) 1030°C and (b) 1150°C: (Z) ZnO grain; (T) $Bi_4Ti_3O_{12}$; (B) Bi-rich grain boundary; (S) Zn_2TiO_4 spinel grain.

Table 2
Electrical measurements for $ZnO{\cdot}Bi_2O_3{\cdot}CoO{\cdot}MnO{\cdot}TiO_2$ varistor system

Sintering		Relative density (%)	Grain size (μm)	Breakdown voltage (E_b, V mm^{-1})
Temp. (°C)	Time (h)			
1150	1	95.9	25.4	65
1150	6	93.4	35.7	44
1200	1	95.6	32.0	54
1200	6	93.2	42.3	40
1250	1	94.5	34.4	43
1250	6	92.0	44.7	30
1300	1	93.9	35.8	35
1300	6	91.7	46.1	28

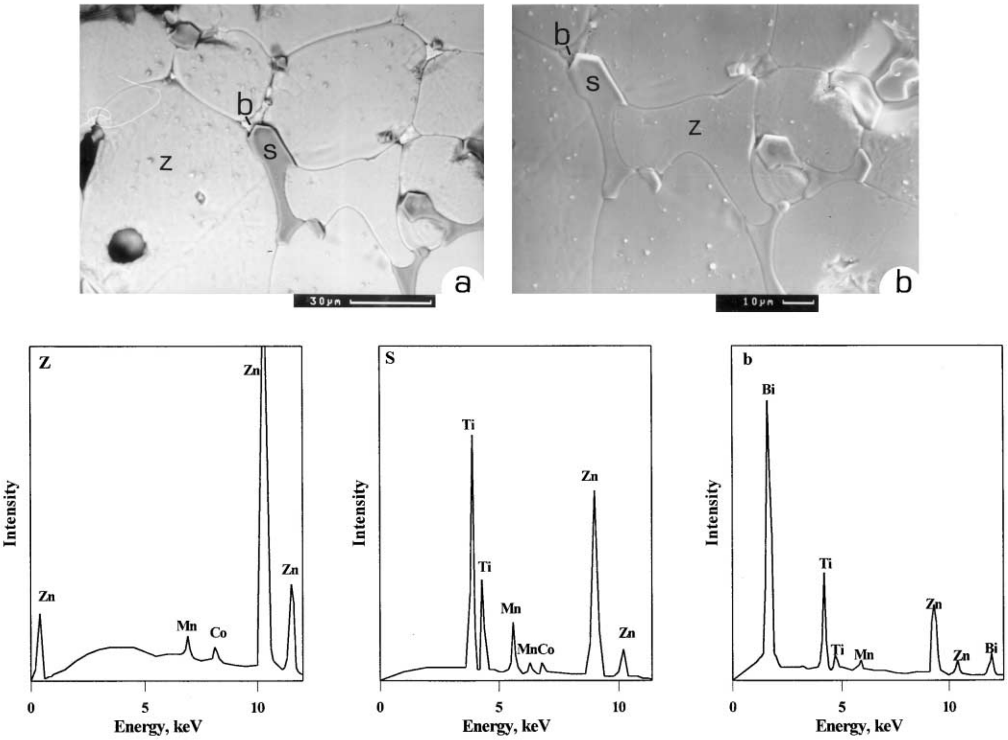

Fig. 5. Backscattered electron SEM image of pellet sintered 6 h at 1150°C: EDS analyses of various features are shown (a) and SEI (b).

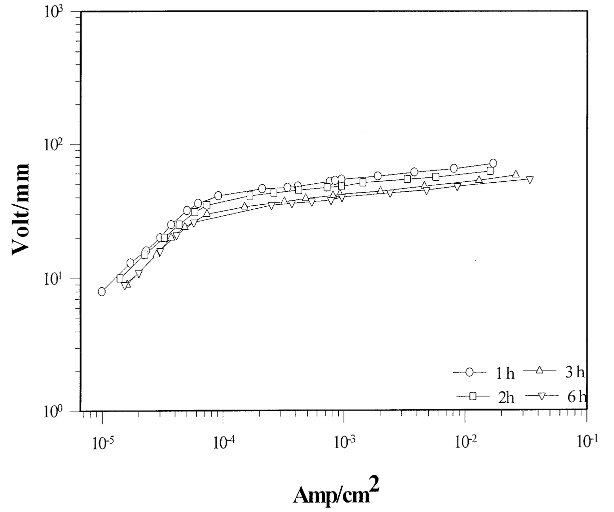

Fig. 6. *E–J* characteristics of ZnO·Bi_2O_3·CoO·MnO·TiO_2 varistor system sintered at 1200°C.

by formation of the liquid Bi_2O_3 and Zn_2TiO_4 spinel [(b) in Fig. 4].

Fig. 5 is a higher magnification backscattered electron SEM image of a sample sintered for 6 h at 1150°C revealing the dark grey Zn_2TiO_4 spinel phase with the lighter grey ZnO grains and white Bi_2O_3 phases located at grain junctions as confirmed by the EDS spectra (Fig. 5).

The electrical response (Table 2 and Fig. 6) of varistors is produced from coprecipitated powder. The samples given a lower sintering temperature and shorter time have higher E_b value because of smaller grain size. This reported work on the densification process of ZnO·Bi_2O_3·MnO·CoO·TiO_2 system showed decrement in the % relative density data with increasing sintering temperature and time (Table 2). This was attributed to the entrapment of gas giving rise to closed pores in ZnO grains and also to the Bi_2O_3 losses due to volatilisation [15].

4. Conclusions

Homogeneous low voltage ZnO varistor powder prepared by chemical processing and single step has been successfully fabricated. Submicrometer particles result from the process, consisting of an intimate mix of ZnO, Zn_2TiO_4 spinel phase and Bi_2O_3 phases.

References

[1] L.M. Levinson, H.R. Philipp, Zinc oxide varistor — a review, Ceram. Bull. 65 (4) (1986) 639–646.
[2] M. Matsuoka, Nonohmic properties of zinc oxide, Japanese J. Appl. Phys. 10 (6) (1971) 736–746.
[3] L.M. Levinson, H.R. Philipp, The physics of metal oxide varistors, J. Appl. Phys. 46 (1975) 1332–1341.
[4] Y. Karakaş, W.E. Lee, Processing and phase evolution in ZnO varistor prepared by oxide coprecipitation, Br. Ceram. Trans. 93 (2) (1994).
[5] T.K. Gupta, Application of zinc oxide varistor, J. Am. Ceram. Soc. 73 (7) (1990) 1817–1840.

[6] S.A. Pianaro, P.R. Bueno, E. Longo, J.A. Varela, Microstructure and electric properties of a SnO_2 based varistor, Ceram. Int. 25 (1999) 1–6.

[7] D.F.K. Hennings, R. Hartung, P.J.L. Reijnen, Grain size control in low-voltage varistors, J. Am. Ceram. Soc. 73 (3) (1990) 645–648.

[8] D.R. Clark, Varistor ceramics, J. Am. Ceram. Soc. 82 (3) (1999) 485–502.

[9] Ö. Toplan, V. Günay, O.T. Özkan, Grain growth in the MnO added ZnO-6wt%Sb_2O_3 ceramics system, Ceram. Int. 23 (1997) 251–255.

[10] G. Svehla, Vogel's Quantitative Inorganic Analysis, 6th Edition, Longmans, 1990.

[11] M. Farnsworth, C.H. Kline, Zinc Chemical, 1st Edition, Zinc Development Association, 1973.

[12] G.Y. Sung, C.H. Kim, Anisotropic grain growth of ZnO grain in the varistor system ZnO–Bi_2O_3–MnO–TiO_2, Adv. Ceram. Mater. 3 (6) (1988) 604–606.

[13] H. Suziki, R.C. Bradt, Grain growth of ZnO in ZnO–Bi_2O_3 ceramics with TiO_2 additional, J. Am. Ceram. Soc. 78 (5) (1995) 1354–1360.

[14] A. Peigney, H. Andrianjatovo, R. Legros, A. Rousset, Influence of chemical composition on sintering of bismuth–titanium-doped zinc oxide, J. Mater. Sci. 27 (1992) 2397–2405.

[15] O.T. Özkan, M. Avci, E. Oktay, H. Erkalfa, Grain growth in MnO-added ZnO–6%wt% Bi2O3 ceramic system, Ceram. Int. 24 (1998) 151–156.